atmosphere

MDPI

Article

Comparison of Atmospheric Circulation Anomalies between Daytime and Nighttime Extreme High Temperature in North China

Peng Chen [1], Gang Zeng [1,*], Xiaoye Yang [1] and Vedaste Iyakaremye [2]

[1] Key Laboratory of Meteorological Disaster of Ministry of Education (KLME), Collaborative Innovation Center on Forecast and Evaluation of Meteorological Disasters (CIC–FEMD), Nanjing University of Information Science and Technology, Nanjing 210044, China
[2] Rwanda Meteorology Agency, Kigali 20093, Rwanda
* Correspondence: zenggang@nuist.edu.cn

Abstract: Many previous studies have shown that atmospheric circulation anomalies are usually the direct cause of extreme high temperatures (EHT). However, the atmospheric circulation anomalies associated with daytime and nighttime EHTs in North China and their differences are less discussed. The present study divides the summer EHTs in North China into independent daytime EHT (ID-EHT) and independent nighttime EHT (IN-EHT) according to the 90th percentile thresholds of the daily maximum and minimum temperature from CN05.1 and compares their atmospheric circulation anomalies. Composite results show that the sinking motion anomaly over North China and the southward displacement of the Western Pacific Subtropical High (WPSH) cause less low cloud cover and water vapor, which is conducive to absorbing more solar radiation at the surface, and leads to the daytime high temperature of ID-EHT. With the disappearance of solar radiation at night, the heat is rapidly dissipated, and the high temperature cannot be maintained. A wave train from high latitudes can affect ID-EHT weather. On the contrary, the upward motion anomaly over North China cooperates with the northward displacement of the WPSH, leading to more clouds and water vapor over North China. As a result, the absorption of solar radiation in North China during the daytime is reduced, and EHT has difficulty in forming during the day. The higher humidity causes slower heat loss from daytime to nighttime, resulting in an IN-EHT. IN-EHT is more likely to be affected by a wave train such as the Silk Road pattern from the midlatitudes.

Keywords: independent daytime extreme high temperature; independent nighttime extreme high temperature; atmospheric circulation anomaly; mechanism

check for updates

Citation: Chen, P.; Zeng, G.; Yang, X.; Iyakaremye, V. Comparison of Atmospheric Circulation Anomalies between Daytime and Nighttime Extreme High Temperature in North China. *Atmosphere* **2023**, *14*, 495. https://doi.org/10.3390/atmos14030495

Academic Editors: Er Lu, Qingchen Chao and Hui Wang

Received: 5 February 2023
Revised: 1 March 2023
Accepted: 1 March 2023
Published: 3 March 2023

Copyright: © 2023 by the authors. Licensee MDPI, Basel, Switzerland. This article is an open access article distributed under the terms and conditions of the Creative Commons Attribution (CC BY) license (https://creativecommons.org/licenses/by/4.0/).

1. Introduction

Extreme high temperature (EHT) events occur more frequently under sustained global warming, posing more serious threats to human health, social, and economic development [1–6]. For example, sustained EHT events can lead to forest fires (Matsueda et al., 2011). In addition, EHT increases power system load, affecting industrial production [7,8]. More importantly, the frequent occurrence of EHT events at night can increase the frequency of diseases such as heat stroke and can increase the incidence of respiratory and cardiovascular diseases [9–12].

North China is a climate-sensitive region, and its daily maximum temperature (Tmax) and daily minimum temperature (Tmin) increased sharply after the 1990s [13]. Many studies explored the causes of EHT in North China [14,15]. The anomaly of the anticyclone circulation in the middle troposphere over North China is the most direct cause of the EHT [15,16]. The anticyclone causes adiabatic heating through an anomalous sinking motion and disperses clouds over North China, reducing water vapor and thereby increasing the solar radiation on the surface to heat the surface [13,17,18]. Meanwhile, the poleward

displacement of the East Asian westerly jet stream (WJS) in the upper troposphere could also contribute to the EHT in North China [19]. Ding et al. [20] found that when WJS is located to the north, it will lead to an abnormally northerly anticyclone, which will increase the EHT in the north. When WJS is weakened, the East Asian monsoon will weaken, leading to weak water vapor content transported in North China. In addition, the teleconnection circulation in the mid-high latitudes of Eurasia and the western Pacific subtropical high (WPSH) in summer are the main backgrounds affecting the EHT in North China [21]. In addition to circulation patterns, solar radiation, aerosols, clouds, water vapor transport, and evaporative feedback also contribute to the onset and persistence of EHT [17,22].

Unlike daytime EHT, nighttime EHT has the property of high humidity, which can prevent heat dissipation at night through the greenhouse effect and maintain a high Tmin [23]. For example, EHT at night in South China is caused by the abnormal southerly wind, which significantly enhances the water vapor flux transport to South China, thereby increasing the air humidity, while the daytime EHT is accompanied by the abnormal northerly wind and extremely low humidity [24].

Previous definitions of EHT in North China only considered extreme maximum or minimum temperatures [13,18,25]. Therefore, the analysis results are mainly related to daytime (nighttime) EHT and include some nighttime (daytime) EHT signals. The definition of univariate hinders our ability to understand the physical mechanisms that are intrinsically different between daytime and nighttime extreme heat, which can cause the process-based weather forecasts and associated heat alerts to deviate from the correct type of event. Therefore, it is necessary to use a bivariate definition to distinguish between high temperatures during the day and at night to improve our understanding of the differences in circulation, dynamics, and thermodynamic mechanisms of these two types of high temperatures.

In this paper, we analyze the circulation differences and dynamic thermal differences between the two types of EHT that occur only during the day and at night, as well as the circulation differences between the day and night for each EHT. This not only explains the different reasons for the occurrence of the two types of EHT but also elucidates why EHT do not occur at night (daytime) when EHT occur only during the day (night). The rest of this paper is organized as follows: Section 2 presents the data and methods. Then, the main results are presented in Section 3, followed by the main conclusions and discussions in Section 4.

2. Data and Methods

2.1. Data

The temperature data used in this study include the daily maximum temperature (Tmax) and daily minimum temperature (Tmin) from CN05.1 datasets [26] with a horizontal resolution of 0.25° × 0.25° from 1979 to 2019. In addition, ERA5 hourly datasets, including Geopotential height, three-dimensional wind, relative humidity, specific humidity, total cloud cover, surface net longwave radiation flux (down is positive), surface net shortwave radiation flux (down is positive), surface 2 m temperature, and surface sensible heat flux (upward is positive) from 1979 to 2019 with a horizontal resolution of 0.25° × 0.25° released by the European Center for Medium-Range Weather Forecasting are also used in this study.

2.2. Definition of EHT

In this paper, the relative threshold is used to define EHT in summer (the summer in this study is defined as June–August). The threshold is calculated by the regional average. These EHTs in North China (35°–45° N, 110°–120° E) are classified into independent daytime EHT (ID-EHT) and independent nighttime EHT (IN-EHT) types based on the following three requirements. ID-EHT type: (1) Tmax > 90th percentile threshold on the current day. (2) Tmin < 90th percentile threshold on the current day. (3) Tmin < 90th percentile threshold on the next day. IN-EHT type: (1) Tmax < 90th percentile threshold on the current day. (2) Tmin > 90th percentile threshold on the next day. (3) Tmax < 90th percentile threshold on the next day [27]. ID-EHT means that EHT occur only during the day but

not at night. IN-EHT means that high temperatures occur only at night but not during the day. The purpose of this definition is to distinguish between signals of high daytime temperatures and high nighttime temperatures.

Since the minimum temperature recorded by CN05.1 is about two o'clock every day, we use the next day's minimum temperature to represent the current night's minimum temperature. Meteorological data collected at 0600 UTC (14:00 Beijing time) is used to describe dynamic-thermal conditions for daytime maximum temperatures, while data collected at 1800 UTC (02:00 Beijing time) is used to describe dynamic-thermal conditions for minimum nighttime temperatures.

To consider cases as much as possible, and thereby improve statistical significance, we performed a composite analysis of 194 regional ID-EHT and 184 IN-EHT, instead of a composite analysis of EHT events, for at least three consecutive days. Anomalies on EHT days are obtained by subtracting the multi-year averages of the corresponding calendar days, indicating that the seasonal climatic cycle was removed. In addition, we selected 14:00 on the day when the EHT occurred and 2:00 am on the next day to analyze the evolution of the circulation in one day. The average value of 1979–2019 is selected as the average climatic result.

3. Results

3.1. Local Temperature and Circulation Anomalies

To understand the causes of ID-EHT and IN-EHT comprehensively, the local temperature and atmospheric circulation anomalies associated with those extremes are first investigated. Figure 1 depicts the composite Tmax and Tmin anomalies for ID-EHT and IN-EHT. When an ID-EHT occurs, a positive temperature anomaly in North China is stronger during the daytime than at nighttime (Figure 1a,c), suggesting that the ability of daytime high temperatures to persist into the night is poor, so that EHT could not occur at night. Contrary to the ID-EHT, IN-EHT nighttime temperature anomaly is stronger than the daytime temperature anomaly (Figure 1b,d), which indicates that the daytime temperature's ability to persist during the night is strong so that EHT occurs at night. In addition, the daytime temperature anomaly of ID-EHT is stronger than that of IN-EHT (Figure 1a,b), but the nighttime temperature anomaly of ID-EHT is weaker than that of IN-EHT (Figure 1c,d). In general, ID-EHT has a faster heat dissipation from day to night, while IN-EHT has a slower heat dissipation from day to night. Therefore, the daytime heating rate of ID-EHT was faster than that of IN-EHT, and the nighttime cooling rate of ID-EHT was faster than that of IN-EHT. To understand the reasons for the difference in daytime and nighttime temperature anomalies between the two types of EHTs and their respective daytime and nighttime temperature anomalies, local thermal factors and humidity conditions are first investigated.

Shortwave radiation plays a major role in the Earth's climate system because it is a key component of the energy balance at the surface. It has important implications for water vapor evaporation, cloud formation, climate, and climate change [28]. When an ID-EHT occurs, the surface net short-wave radiation flux (SNSWRF) and the surface sensible heat flux (SSHF) in North China is a positive anomaly during the daytime (Figure 2a), which indicates that the surface absorbs more solar radiation and the surface transports more sensible heat flux to the atmosphere than at other times of the climate during the daytime. Sensible heat flux from the surface to the atmosphere and positive anomalies of solar radiation during the daytime act as a heat source for heating the surface, resulting in a rapid rise of surface air temperature (SAT) and a positive anomaly during the daytime (Figure 2a). However, as the short-wave solar radiation disappears at nighttime, and so does the heat source at night. At nighttime, the SSHF in North China is negative (Figure 2c), which indicates that the atmosphere is warmer than the surface, and the atmosphere can better transfer heat to the surface to achieve the cooling effect. In addition, the surface net long-wave radiation flux (SNLWRF) is a negative anomaly (Figure 2c), which leads to a more rapid loss of surface heat and a decrease in the surface temperature anomaly. IN-EHT is different from ID-EHT. When the IN-EHT occurs, the SNSWRF in North China

is a negative anomaly during the daytime (Figure 2b), which means the heating effect of solar radiation on the surface and atmosphere is obviously weakened. The negative anomalous SSHF also shows that the sensible heat flux from the North China surface to the atmosphere decreases, which is lower than the climate state level (Figure 2b). A heat source below the climate level causes IN-EHT daytime temperature anomalies in North China during the daytime to be smaller than ID-EHT daytime temperature anomalies (Figure 2a,b). The positive anomalous SNLWRF and SSHF (Figure 2d) that indicate the sensible heat flux from the atmosphere to the surface is weakened and slows down the rate of nighttime temperature reduction on the surface in North China. As a result, the nighttime temperature anomaly of the IN-EHT is much stronger than that of the ID-EHT ((Figure 2c,d).

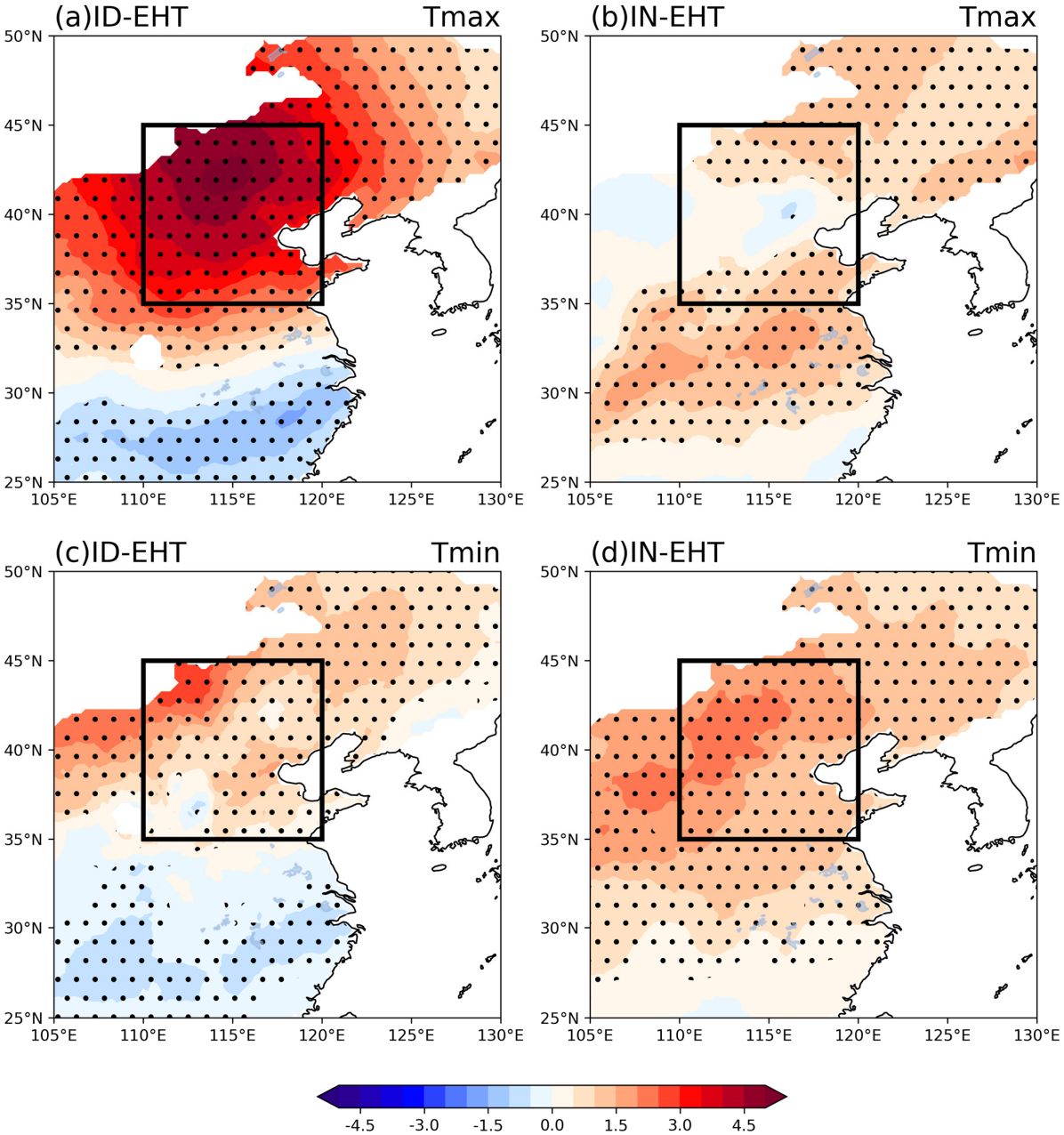

Figure 1. Composite anomalies of Tmax for (**a**) ID-EHT, (**b**) IN-EHT; (**c**,**d**): the same as (**a**,**b**) but for Tmin anomalies (shading; units: °C). Black dots indicate the anomalies significant at the 95% confidence level.

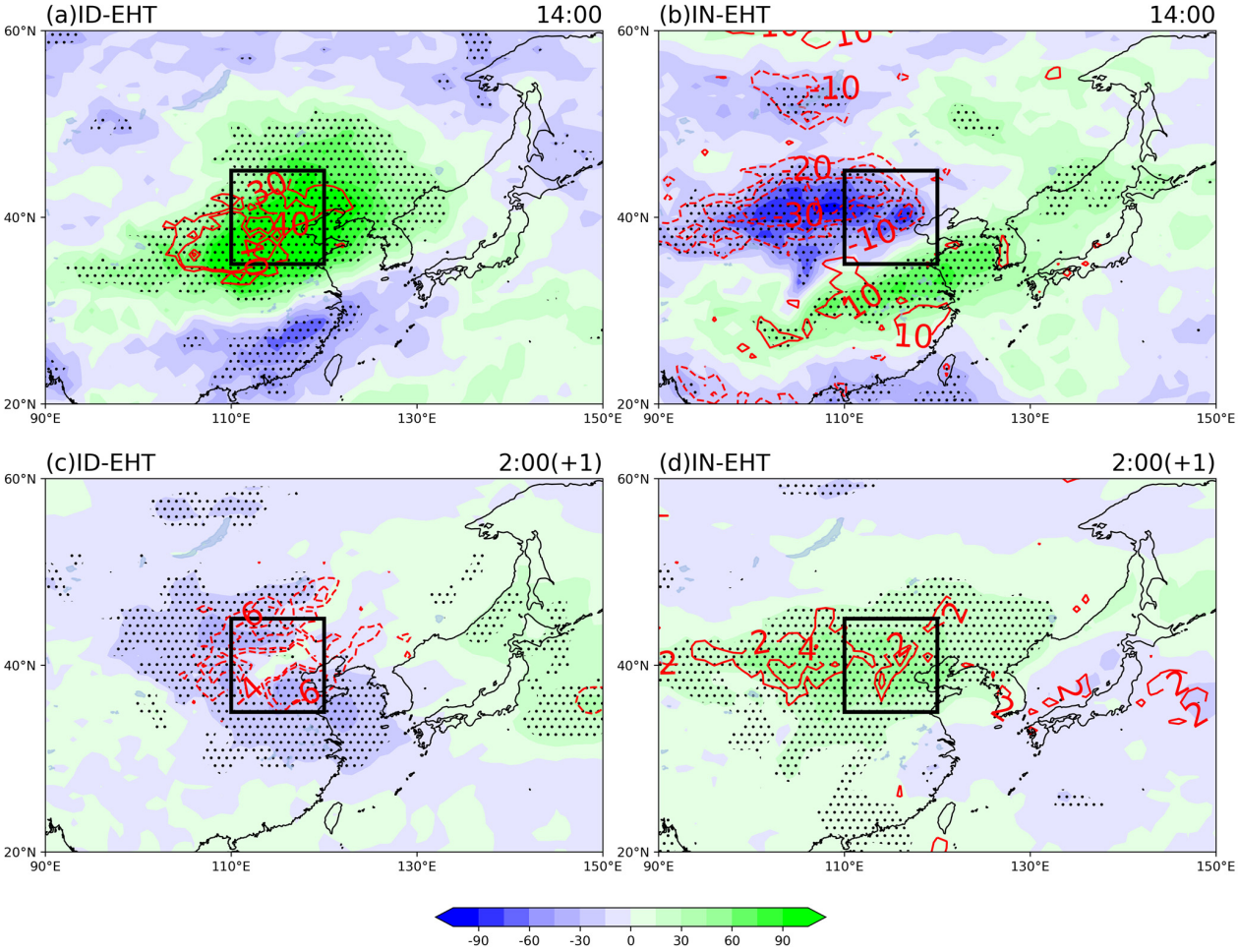

Figure 2. Composite anomalies of surface net short-wave flux (shading; units: W/m^2) at 14:00 (**a**) and surface net long-wave radiation flux (shading; units: W/m^2) at 2:00 of the next day (**c**) for ID-EHT; (**b**,**d**) are same as (**a**,**c**) but for IN-EHT. The red solid and dotted contours represent surface sensible heat flux anomalies with 10 intervals in (**a**,**b**) and 2 intervals in (**c**,**d**). Black dots indicate the anomalies significant at the 95% confidence level.

Dai et al. [29] found that clouds can reduce the diurnal temperature range by 25–50% compared with clear-sky days over land areas. Clouds play a vital role in blocking, absorbing, and reflecting solar radiation [30]. They directly determine how much solar radiation the surface can absorb and act as a layer of insulation. Figure 3a,c show that when an ID-EHT occurs, a negative anomaly of cloud cover exists in North China during daytime and nighttime. The negative cloud cover anomalies during daytime indicate that the cloud cover amount is less, and more solar radiation is absorbed by the surface, which leads to an increase in positive temperature anomalies. Due to the decrease in cloud cover, SNLWRF decreases, and the insulation effect of the clouds at nighttime is weakened, which results in the positive temperature anomaly at night. However, there is a positive cloud cover anomaly over North China during daytime and nighttime (Figure 3b,d) when an IN-EHT occurs. The cloud cover over North China during the daytime blocks a large amount of solar radiation, and the solar radiation reaching the surface is limited, which results in a lower positive temperature anomaly. At nighttime, the spatial extent and amount of cloud cover increases again, leading to the increase in SNLWRF, enhancing cloud insulation, and a higher positive temperature anomaly [31].

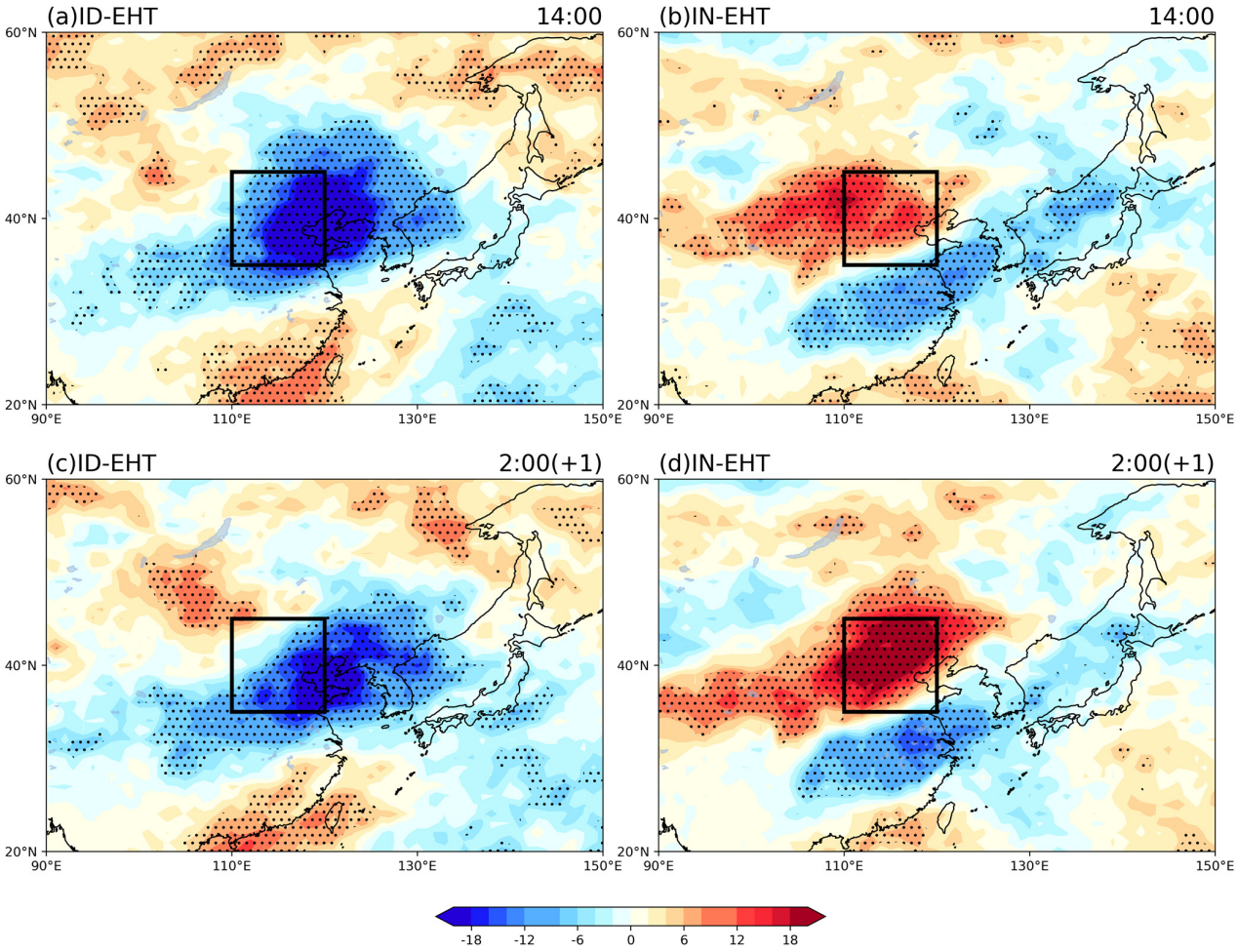

Figure 3. Composite anomalies of total cloud cover (shading; units: %) at 14:00 (**a**) and at 2:00 of the next day (**c**) for ID-EHT; (**b**,**d**) are same as (**a**,**c**) but for IN-EHT. Black dots indicate the anomalies significant at the 95% confidence level.

Water vapor is a greenhouse gas that can increase daytime and nighttime temperatures by storing large amounts of heat [29]. It can be seen from Figure 4a,c that when an ID-EHT occurs, the specific humidity (SH) of 850 hPa over North China is a negative anomaly, indicating that there is less water vapor over North China at this time. Judging from the water vapor flux of 850 hPa, the water vapor mainly comes from the Bay of Bengal. During the daytime, the water vapor content in the atmosphere over North China is low, which is beneficial for the surface to absorb solar radiation to heat the surface air. At night, the heat of the surface is more easily diffused and lost due to the drying of the air (Figure 4c). Due to the low water vapor content in the atmosphere during the daytime, the atmosphere can only store a small amount of heat, which cannot maintain the temperature of the atmosphere during the day well into the night, resulting in a low night positive temperature anomaly (Figure 1c). However, when the IN-EHT occurs, the positive anomalous SH over North China represents more water vapor in the North China atmosphere at this time (Figure 4b). From the perspective of 850 hPa water vapor flux, the main water vapor comes from the Bay of Bengal and the western Pacific (Figure 4b). More water vapor in the daytime can store a lot of energy in the atmosphere, which can reduce the cooling rate from daytime to nighttime and more effectively maintain the heat of the atmosphere in the daytime, resulting in a higher positive temperature anomaly at night.

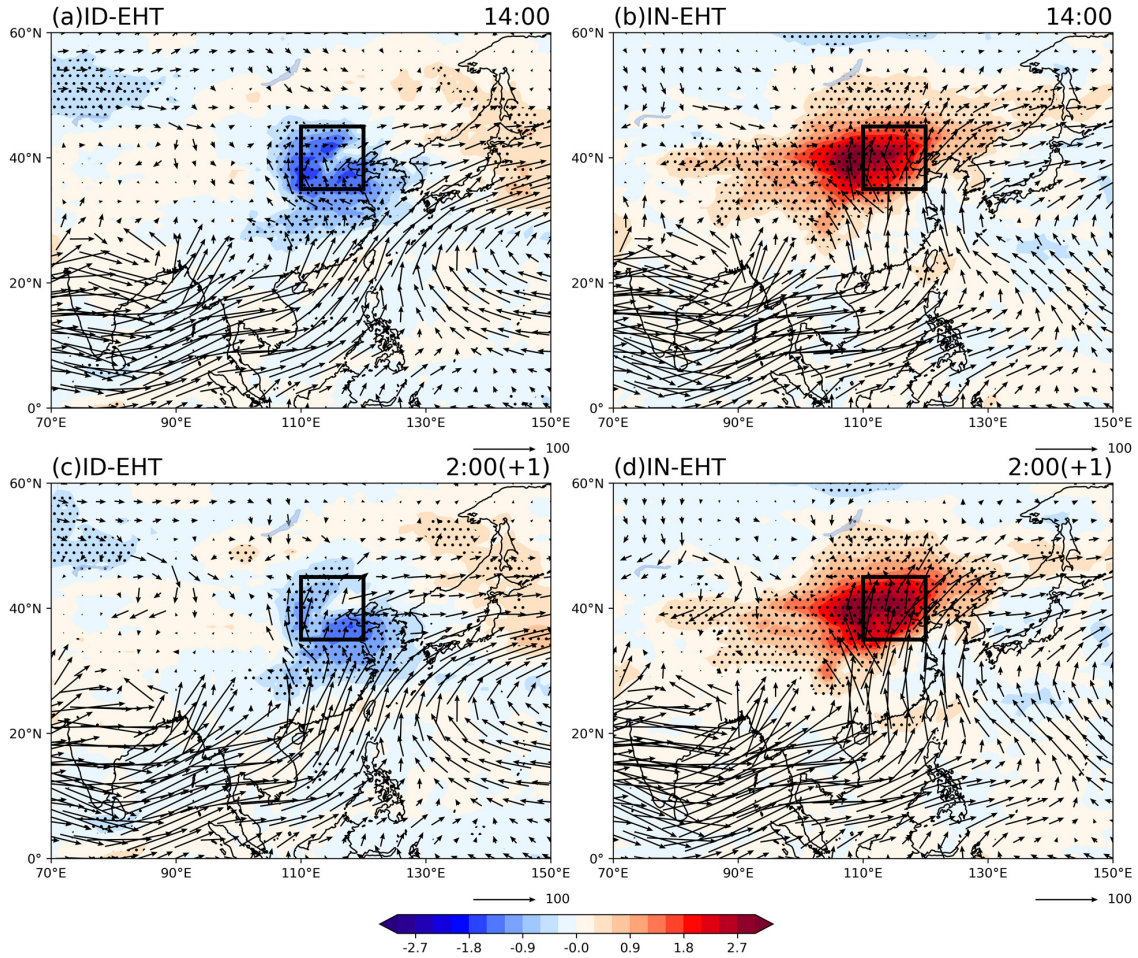

Figure 4. Composite anomalies of 850 hPa specific humidity (shading; unit: g/kg) and water vapor flux (arrows; unit: (m·g)/(s·kg)) at 14:00 (**a**) and at 2:00 of the next day (**c**) for ID-EHT; (**b**,**d**) are same as (**a**,**c**) but for IN-EHT. Black dots indicate the anomalies significant at the 95% confidence level.

3.2. Large-Scale Circulation Anomalies and Their Evolutions

Because there is little difference in large-scale circulation between 14:00 and 2:00 in the ID-EHT or IN-EHT, each type of EHT only gives one time period for analysis in this section, with ID-EHT occurring at 14:00 and IN-EHT occurring at 2:00. To understand the causes of these two extreme high temperatures further, large-scale circulation anomalies associated with ID-EHT and IN-EHT and their evolution are also investigated. Figure 5a shows that when an ID-EHT occurs, a consistent subsidence movement exists from the upper to lower troposphere over North China during the daytime. The sinking motion is not conducive to the accumulation of water vapor and reduces the cloud cover amount. In addition, the ascending motion over South China and the subsiding motion over the South China Sea constituted the third-order circulation with the subsiding motion over North China, which was conducive to the strengthening and maintenance of the subsiding motion over North China. When an IN-EHT occurs, a rising movement over North China (Figure 5b) is conducive to the accumulation of cloud volume and water vapor. The subsiding motion over the middle and lower reaches of the Yangtze River and the ascending motion over the South China Sea constitute the third-order circulation with the ascending motion over North China, which is conducive to the strengthening and maintenance of the ascending motion over North China.

There is an anticyclone anomaly over North China, a cyclone anomaly over South China, and an anticyclone in the southeastern part of North China in the upper troposphere when an ID-EHT occurs (Figure 6a). With the cooperation of such a wind anomaly, water

vapor transport from the sea to North China is blocked, resulting in a negative SH anomaly over North China (Figure 4a), indicating that North China is relatively dry. Figure 6b shows that when an IN-EHT occurs, an anticyclone dominates over North China. The spatial scope and intensity of the anticyclones are larger than those of ID-EHT. Its south side extends to South China, and the original cyclone disappears. Under the control of such a wind anomaly, a larger amount of water vapor from the sea surface can be transported to North China, which is conducive to the formation of a stable moisturizing layer over North China during the day.

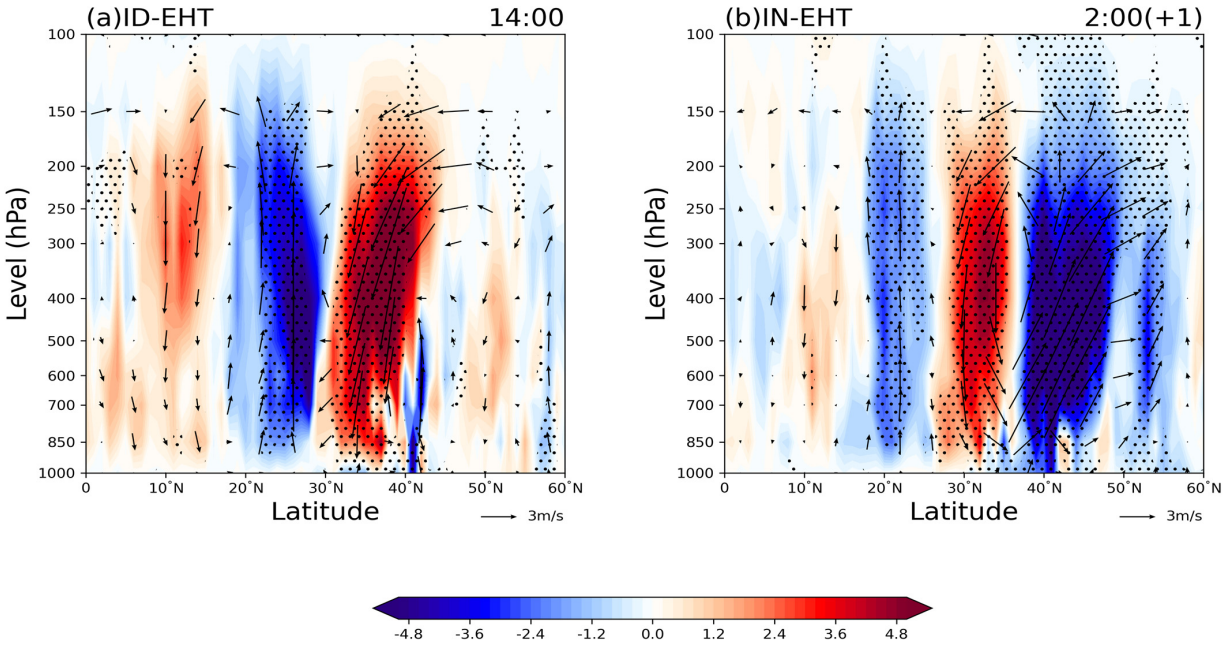

Figure 5. Composite anomalies of meridional vertical winds (arrows, units: pa/s, averaged from 110° E to 120° E, the vertical component is amplified 100 times) and vertical motion (shading, units: pa/s) at 14:00 (**a**) for ID-EHT and at 2:00 (**b**) on the next day for IN-EHT. Black dots indicate the anomalies significant at the 95% confidence level.

Some studies [32,33] have suggested that water vapor transport in North China is closely related to the location of the WPSH. Figure 7a shows that North China is located at the front of the anticyclone in the middle troposphere and the northeasterly wind anomalies occur when an ID-EHT occurs. In addition, there is a cyclone anomaly to the south of North China and an anticyclone anomaly to its southeast. The southward WPSH is not conducive to the western Pacific water vapor transport to North China. When the IN-EHT occurs, although the sky over North China is also controlled by an anticyclone anomaly in the middle troposphere, North China is located at the rear of the anticyclone anomaly and has a strong southerly wind anomaly (Figure 7b). The northward WPSH is conducive to the transport of the western Pacific water vapor to North China.

Previous studies have suggested that the WJS in the mid-latitudes is closely related to vertical motion and changes in cloud cover that may affect radiation and precipitation, ultimately leading to temperature changes [7,34]. Figure 8a shows that a pair of cyclones–anticyclones anomalies are controlled over North China at 200 hPa, and the northeasterly wind anomaly weakens the intensity of the WJS when the ID-EHT occurs. However, an anticyclone anomaly dominates North China, and the southwesterly winds from the anomalous anticyclone strengthen WJS when the IN-EHT occurs (Figure 8b). The weakening (strengthening) of the WJS also played a crucial role in the weakening (strengthening) of the East Asian summer monsoon [32]. As a result, the water vapor transported and converged by the East Asian summer monsoon to the north was greatly weakened (strengthened), resulting in a serious shortage (plenty) of water vapor supply for precipitation in North China.

When an ID-EHT or IN-EHT occurs, WJS is located in different locations in North China. The former is located in the southeast of North China and the latter in the northwest of North China. This is consistent with previous studies [35–37]. For example, Zhou et al. [37] found that the centers of the dominant mode of the WJS in late summer extend more to the west and north than in early summer.

Figure 9 shows the evolution of the geopotential height anomaly and the wave action flux anomaly at 200 hPa for the ID-EHT and IN-EHT. There are different atmospheric teleconnections between the two types of EHT. When an ID-EHT occurs, a "- + -" geopotential height anomaly wave train appears over the Eurasian continent (Figure 9d). Two negative centers are located over the Barents Sea and the Kara Sea to Siberia and South China, while the positive center is over Mongolia. This wave train appeared 6 to 3 days before the onset of EHT and continued to intensify with time before the onset of ID-EHT, and this wave train has a certain similarity with the teleconnection wave train of the blocking EHT in northeast China [38]. The wave action flux that propagated from high latitudes to North China reached the strongest on the day ID-EHT occurred. The center of the negative geopotential height anomaly in the Barents Sea, Kara Sea and Siberia is relatively stable in the process of evolution, and the wave energy propagates southward. As a result, the geopotential height anomaly over North China has been continuously strengthened for 6 days before the occurrence of the ID-EHT to the current day, indicating that the center of the negative geopotential height anomaly may be a potential early signal for the occurrence of ID-EHT. However, the evolution of IN-EHT is also significantly different from that of ID-EHT. The geopotential height anomaly over North China is due to the increasing intensity of the geopotential height anomaly over the Caspian Sea, the Black Sea, and the Mediterranean Sea. Unlike the ID-EHT, the wave train when the IN-EHT occurs mainly comes from the middle latitudes, showing the geopotential height anomaly of "+ - + -" (Figure 9i), which is similar to the Silk Road pattern [39]. The center of negative geopotential height anomaly is located over the Pamir Plateau to the Tianshan Mountains and over the eastern part of Japan. In contrast, the center of positive geopotential height anomaly is located over North China and the Caspian Sea to the Mediterranean Sea, and the positive geopotential height anomaly center over the Caspian Sea to the Mediterranean Sea may be an early prediction signal of the occurrence of the IN-EHT. The wave energy travels eastward and reaches its strongest on the day of the IN-EHT.

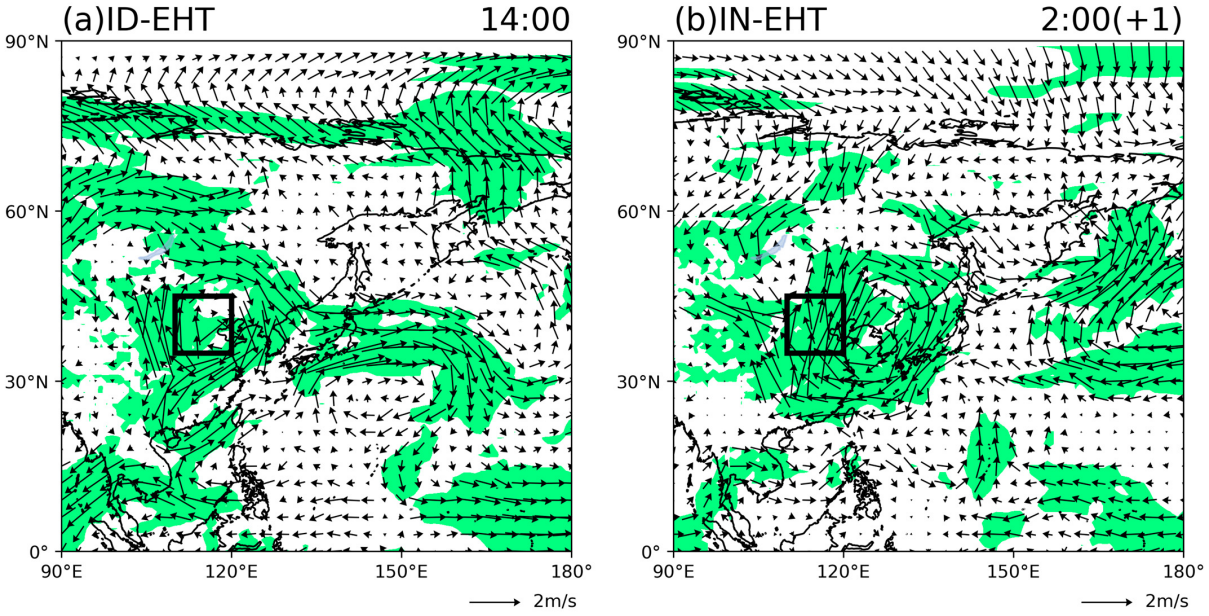

Figure 6. Composite anomalies of 850 hPa wind (arrows; units: m/s) at 14:00 (**a**) on the day for ID-EHT and at 2:00 (**b**) on the next day for IN-EHT. Green shaded areas indicate that either the zonal or meridional wind anomalies are significant at the 95% confidence level.

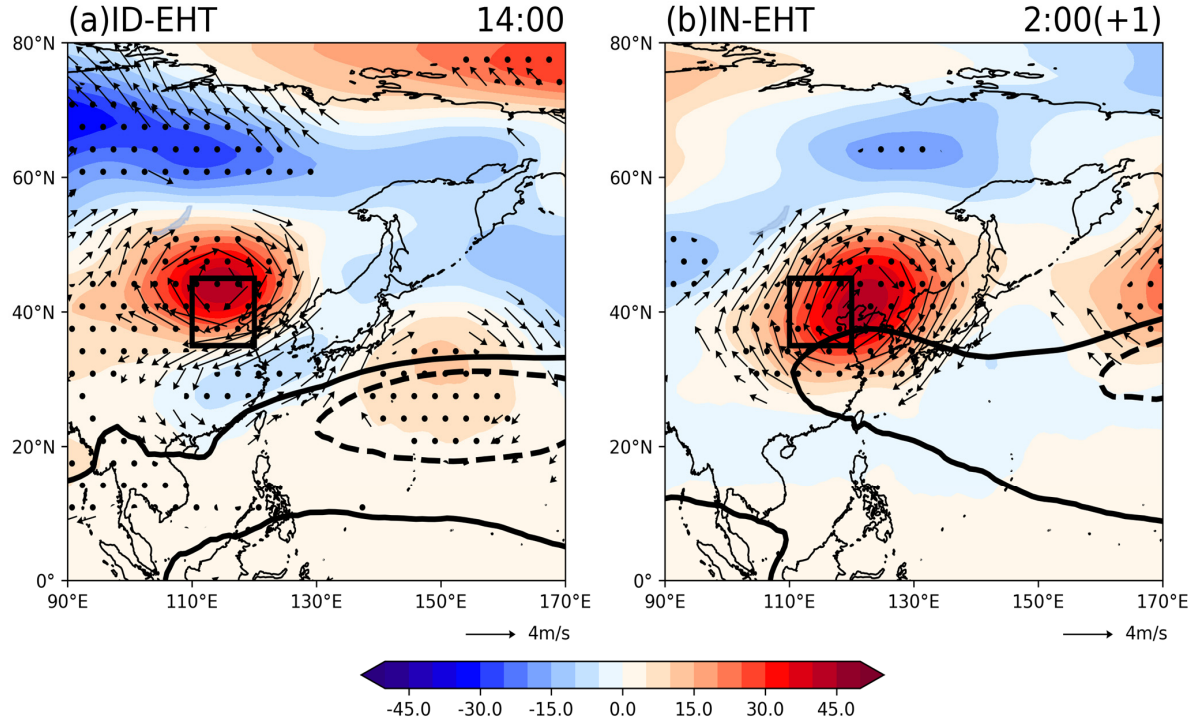

Figure 7. Composite anomalies of 500 hPa wind (arrows; units: m/s) and geopotential height (shading; units: m) at 14:00 (**a**) on the day for ID-EHT and at 2:00 (**b**) on the next day for IN-EHT. The black solid and dotted contours represent the WPSH domain (depicted by geopotential height of 5860 and 5880 m); Only wind anomalies that are significant at the 95% confidence level are retained.

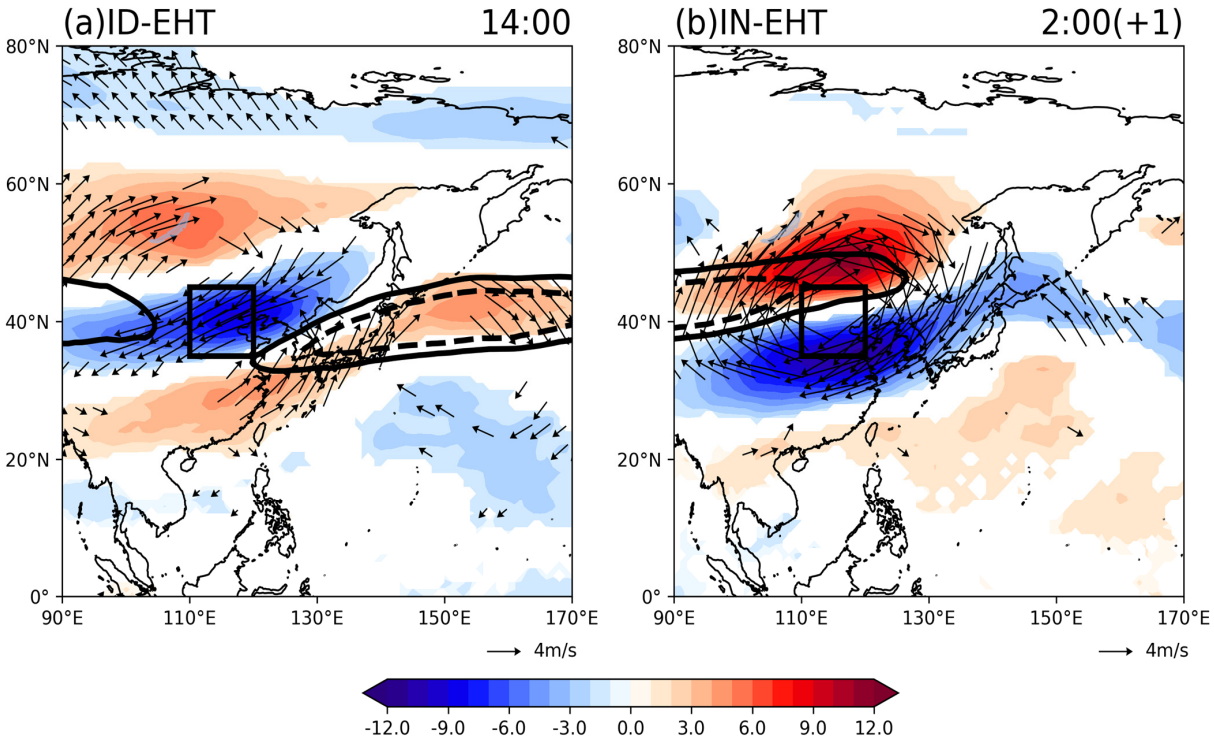

Figure 8. Composite anomalies of 200 hPa wind (arrows; units: m/s) and zonal wind (shading, units: m/s) at 14:00 (**a**) on the day for ID-EHT and at 2:00 (**b**) on the next day for IN-EHT. The black solid and dotted contours represent the westerly jet stream domain (depicted by zonal wind speed of 25 m/s and 30 m/s); Only wind anomalies that are significant at the 95% confidence level are retained.

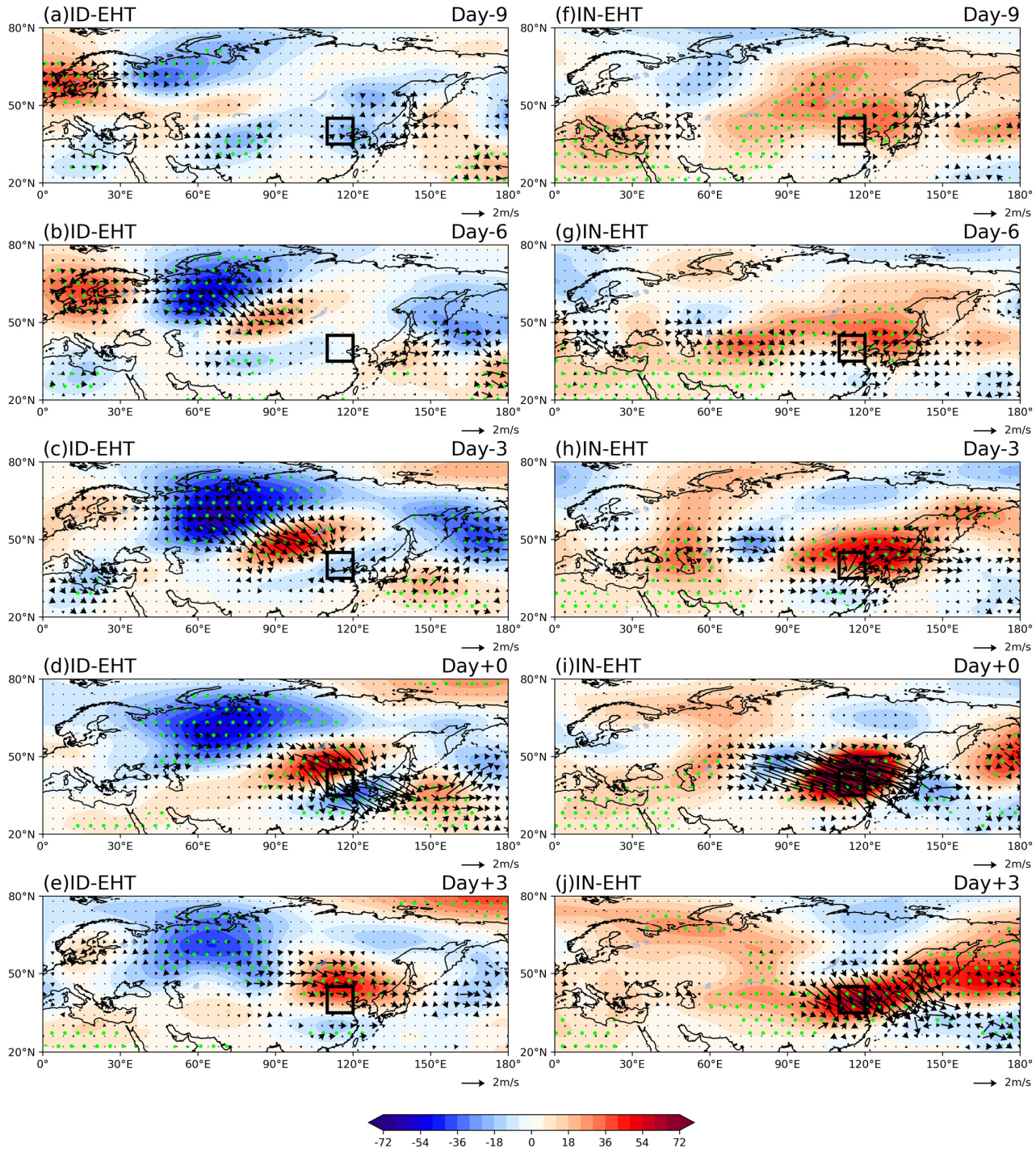

Figure 9. Composite evolution of 200 hPa geopotential height anomalies (shading; units: m) and the 200 hPa wave activity flux (arrows; units: m^2/s^2) (from day −9 to day +3 for (**a**–**e**): ID-EHT, (**f**–**j**): IN-EHT). Green dots indicate the anomalies significant at the 95% confidence level.

4. Conclusions and Discussions

4.1. Conclusions

Using the CN05.1 homogenized observational data of daily maximum and minimum temperature across China during 1979–2019, we divide the summer EHTs in North China into ID-EHTs and IN-EHTs. The daytime temperature anomaly of the IN-EHT is much smaller than that of the ID-EHT. However, the temperature anomaly of the IN-EHT at night is much stronger than that of the ID-EHT. The daytime temperature anomaly of ID-EHT

is stronger than that of night, but the daytime temperature anomaly of IN-EHT is weaker than that of night. These two types of EHT in North China result from different large-scale circulations, moisture transport, and adiabatic heating, which can be summarized schematically in Figure 10.

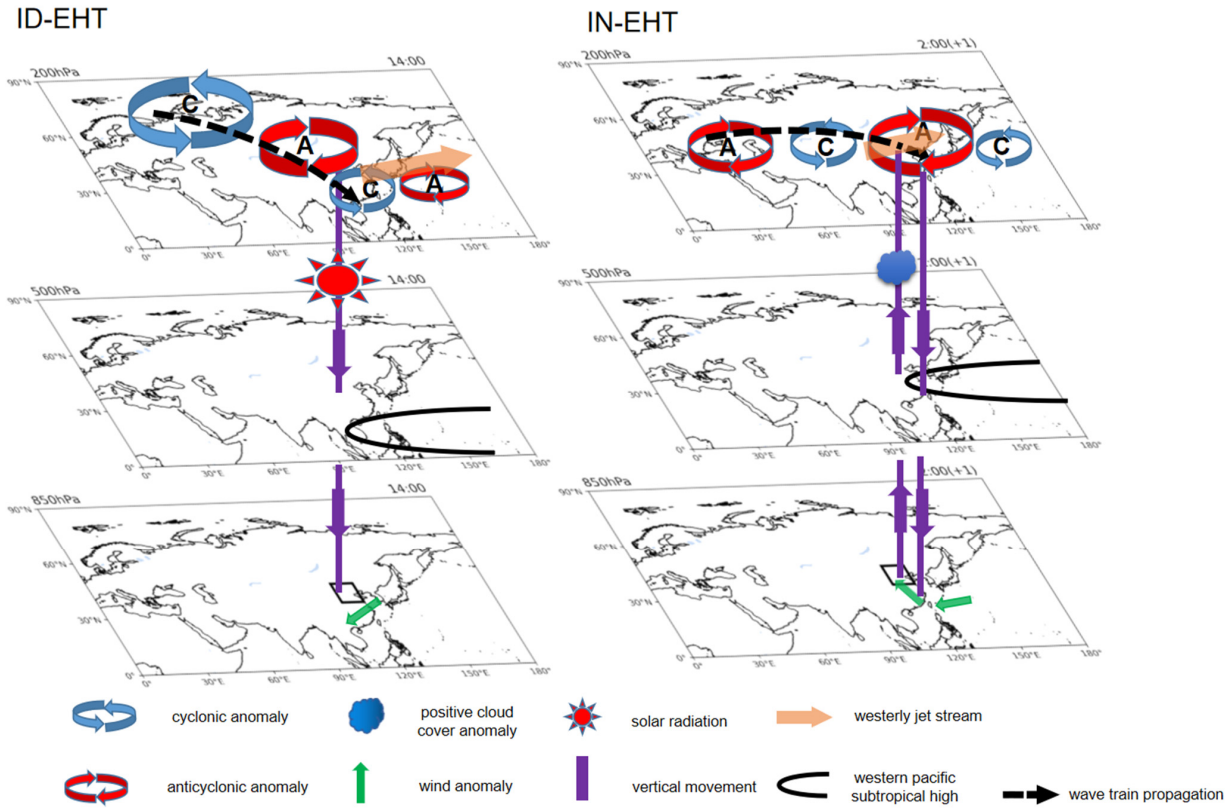

Figure 10. Schematic diagram of circulation anomalies for ID-EHT and IN-EHT in North China.

When an ID-EHT occurs, the wave action fluxes from the high-latitude Barents Sea, Kara Sea, and Siberia spread southward to North China to enhance the anticyclone over North China. The southward WPSH is not conducive to the transport of water vapor from the western Pacific to North China, and a weakened WJS leads to a weakening of the East Asian summer monsoon, which leads to less water vapor delivered by the Bay of Bengal to North China. The south-easterly WJS enhances the sinking movement of the anticyclone, which hampers high temperatures at night. This allows North China to absorb more solar radiation during the daytime, coupled with the sensible heat flux from the surface to the atmosphere, causing the daytime EHT. By night, with the low humidity in North China, the heat at night can be dispersed effectively, so no EHT is formed.

However, when an IN-EHT occurs, a Rossby wave train similar to the Silk Road pattern from the mid-latitude to North China enhances the anticyclone over North China. The northward WPSH brings a large amount of water vapor to North China. The strengthening WJS leads to the strengthening of the East Asian summer monsoon, which leads to an increase in water vapor transported from the Bay of Bengal to North China. The anomalous subsidence movement in the southern part of North China may have stimulated the upward movement in North China, which results in the positive anomaly of water vapor and cloud cover over North China. Clouds over North China reflect a lot of solar radiation, which causes EHT not to occur during the daytime. By night, with the strengthening of the ascending movement, the high humidity in North China is not conducive to heat loss during the day, so the heat continues into the night. Thus, the high temperature at night is formed.

4.2. Discussions

Previous studies have highlighted the importance of WPSH and WJS to EHT in North China. This study further demonstrated that WPSH and WJS exhibited different effects on different types of EHT in North China. The WPSH extends northward (southward) and the WJS extends northwestward (southeastward), and are conducive to the formation of IN-EHT (ID-EHT). Therefore, different predictive factors should be considered to improve the predictive ability of EHT. Mid-high latitude wave trains can be used as signals to predict ID-EHT and IN-EHT, but the mechanism of generating such wave trains is not clear. Possible mechanisms include sea temperature anomalies in the North Atlantic ocean that trigger the wave train, and anomalies in Arctic sea ice cover that trigger the wave train in different north–south directions. In addition, the occurrence of EHT in both day and night in North China has not been explained, which would be an interesting topic.

Author Contributions: Formal analysis, P.C. and G.Z.; writing—original draft, P.C. and G.Z.; writing—review and editing, P.C., G.Z., X.Y. and V.I. All authors have read and agreed to the published version of the manuscript.

Funding: This research is supported by the National Natural Science Foundations of China (42175035) and the National Key Research and Development Program of China (2022YFF0801704).

Acknowledgments: The authors thank the High-Performance Computing Center of Nanjing University of Information Science and Technology for supporting the data processing and visualization of this study.

Conflicts of Interest: The authors declare no conflict of interest.

References

1. McGregor, G.R.; Ferro, C.A.T.; Stephenson, D.B. Projected changes in extreme weather and climate events in Europe. In *Extreme Weather Events and Public Health Responses*; Springer: Berlin/Heidelberg, Germany, 2005; pp. 13–23.
2. Mcmichael, A.J.; Lindgren, E. Climate change: Present and future risks to health, and necessary responses. *J. Intern. Med.* **2011**, *270*, 401–413. [CrossRef]
3. Yatim, A.N.M.; Latif, M.T.; Ahamad, F.; Khan, M.F.; Nadzir, M.S.M.; Juneng, L. Observed Trends in Extreme Temperature over the Klang Valley, Malaysia. *Adv. Atmos. Sci.* **2019**, *36*, 1355–1370. [CrossRef]
4. Pi, Y.; Yu, Y.; Zhang, Y.; Xu, C.; Yu, R. Extreme Temperature Events during 1960–2017 in the Arid Region of Northwest China: Spatiotemporal Dynamics and Associated Large-Scale Atmospheric Circulation. *Sustainability* **2020**, *12*, 1198. [CrossRef]
5. Forster, M.A.; Englefield, A. The water uses and growth response of grapevines to extreme temperature events. *Theor. Exp. Plant Physiol.* **2021**, *33*, 187–203. [CrossRef]
6. Yang, H.Y.; Lee, J.K.W.; Chio, C.P. Extreme temperature increases the risk of stillbirth in the third trimester of pregnancy. *Sci. Rep.* **2022**, *12*, 18474. [CrossRef]
7. Sun, Y.; Zhang, X.; Zwiers, F.W.; Song, L.; Wan, H.; Hu, T.; Yin, H.; Ren, G. Rapid increase in the risk to extreme summer heat in Eastern China. *Nat. Clim. Chang.* **2014**, *4*, 1082–1085. [CrossRef]
8. Su, Y.-W. The Effects of Extreme High Temperature Day Off on Electricity Conservation. *Weather Clim. Soc.* **2021**, *13*, 769–782. [CrossRef]
9. Kovats, R.S.; Hajat, S. Heat stress and public health: A critical review. *Annu. Rev. Public Health* **2008**, *29*, 41–55. [CrossRef]
10. Westcott, N.E. The Prolonged 1954 Midwestern, U.S. Heat Wave: Impacts and Responses. *Weather Clim. Soc.* **2011**, *3*, 165–176. [CrossRef]
11. Campbell, S.; Remenyi, T.A.; White, C.J.; Johnston, F.H. Heatwave and health impact research: A global review. *Health Place* **2018**, *53*, 210–218. [CrossRef]
12. Almendra, R.; Loureiro, A.; Silva, G.; Vasconcelos, J.; Santana, P. Short-term impacts of air temperature on hospitalizations for mental disorders in Lisbon. *Sci. Total Environ.* **2019**, *647*, 127–133. [CrossRef]
13. Zhang, G.; Zeng, G.; Li, C.; Yang, X. Impact of PDO and AMO on interdecadal variability in extreme high temperatures in North China over the most recent 40-year period. *Clim. Dyn.* **2020**, *54*, 3003–3020. [CrossRef]
14. Qian, C.; Zhou, T. Multidecadal Variability of North China Aridity and Its Relationship to PDO during 1900-2010. *J. Clim.* **2014**, *27*, 1210–1222. [CrossRef]
15. Zhang, G.; Zeng, G.; Yang, X.; Iyakaremye, V. Two spatial types of North China heatwaves and their possible links to Barents-Kara Sea ice changes. *Int. J. Climatol.* **2022**, *42*, 6876–6889. [CrossRef]
16. Lu, C.; Ye, J.; Wang, S.; Yang, M.; Li, Q.; He, W.; Qin, Y.; Cai, J.; Mao, J. An Unusual Heat Wave in North China During Midsummer, 2018. *Front. Earth Sci.* **2020**, *8*, 238. [CrossRef]

17. Gershunov, A.; Cayan, D.R.; Iacobellis, S.F. The Great 2006 Heat Wave over California and Nevada: Signal of an Increasing Trend. *J. Clim.* **2009**, *22*, 6181–6203. [CrossRef]
18. Deng, K.; Yang, S.; Ting, M.; Lin, A.; Wang, Z. An Intensified Mode of Variability Modulating the Summer Heat Waves in Eastern Europe and Northern China. *Geophys. Res. Lett.* **2018**, *45*, 11361–11369. [CrossRef]
19. Wang, X.; Zhou, W.; Wang, D.; Wang, C. The impacts of the summer Asian Jet Stream biases on surface air temperature in mid-eastern China in IPCC AR4 models. *Int. J. Climatol.* **2013**, *33*, 265–276. [CrossRef]
20. Ding, Z.; Wang, Y.; Lu, R. An analysis of changes in temperature extremes in the Three River Headwaters region of the Tibetan Plateau during 1961–2016. *Atmos. Res.* **2018**, *209*, 103–114. [CrossRef]
21. Tao, P.; Zhang, Y. Large-scale circulation features associated with the heat wave over Northeast China in summer 2018. *Atmos. Ocean. Sci. Lett.* **2019**, *12*, 254–260. [CrossRef]
22. Freychet, N.; Tett, S.; Wang, J.; Hegerl, G. Summer heat waves over Eastern China: Dynamical processes and trend attribution. *Environ. Res. Lett.* **2017**, *12*, 024015. [CrossRef]
23. Chen, R.; Lu, R. Large-scale circulation anomalies associated with 'tropical night' weather in Beijing, China. *Int. J. Climatol.* **2014**, *34*, 1980–1989. [CrossRef]
24. Lin, W.; Chen, R.; Wen, Z.; Chen, W. Large-scale circulation features responsible for different types of extreme high temperatures with extreme coverage over South China. *Int. J. Climatol.* **2022**, *42*, 974–992. [CrossRef]
25. Chen, R.; Lu, R. Role of Large-Scale Circulation and Terrain in Causing Extreme Heat in Western North China. *J. Clim.* **2016**, *29*, 2511–2527. [CrossRef]
26. Wu, J.; Gao, X. A gridded daily observation dataset over China region and comparison with the other datasets. *Chin. J. Geophys.* **2013**, *56*, 1102–1111.
27. Chen, Y.; Li, Y. An Inter-comparison of Three Heat Wave Types in China during 1961–2010: Observed Basic Features and Linear Trends. *Sci. Rep.* **2017**, *7*, 45619. [CrossRef]
28. Galanaki, E.; Emmanouil, G.; Lagouvardos, K.; Kotroni, V. Long-Term Patterns and Trends of Shortwave Global Irradiance over the Euro-Mediterranean Region. *Atmosphere* **2021**, *12*, 1431. [CrossRef]
29. Dai, A.; Trenberth, K.E.; Karl, T.R. Effects of Clouds, Soil Moisture, Precipitation, and Water Vapor on Diurnal Temperature Range. *J. Clim.* **1999**, *12*, 2451–2473. [CrossRef]
30. Muelmenstaedt, J.; Salzmann, M.; Kay, J.E.; Zelinka, M.D.; Ma, P.-L.; Nam, C.; Kretzschmar, J.; Hörnig, S.; Quaas, J. An underestimated negative cloud feedback from cloud lifetime changes. *Nat. Clim. Chang.* **2021**, *11*, 508–513. [CrossRef]
31. Zhao, W.; Zhang, N.; Sun, J. Spatiotemporal Variations of Cloud Amount over the Yangtze River Delta, China. *J. Meteorol. Res.* **2014**, *28*, 371–380. [CrossRef]
32. Su, T.; Xue, F. The intraseasonal variation of summer monsoon circulation and rainfall in East Asia (in Chinese). *Chin. J. Atmos. Sci.* **2010**, *34*, 611–628.
33. Ge, H.; Zeng, G.; Iyakaremye, V.; Yang, X.; Wang, Z. Comparison of Atmospheric Circulation Anomalies between Dry and Wet Extreme High-Temperature Days in the Middle and Lower Reaches of the Yellow River. *Atmosphere* **2021**, *12*, 1265. [CrossRef]
34. Liang, X.; Wang, W. Associations between China monsoon rainfall and tropospheric jets. *Q. J. R. Meteorol. Soc.* **1998**, *124*, 2597–2623. [CrossRef]
35. Kuang, X.Y.; Zhang, Y.C. Seasonal variation of the East Asian Subtropical Westerly Jet and its association with the heating field over East Asia. *Adv. Atmos. Sci.* **2005**, *22*, 831–840.
36. Lai, X.; Gong, Y.; Cen, S.; Tian, H.; Zhang, H. Impact of the Westerly Jet on Rainfall/Runoff in the Source Region of the Yangtze River during the Flood Season. *Adv. Meteorol.* **2020**, *2020*, 6726347. [CrossRef]
37. Zhou, Y.; Yuan, J.; Wen, Z.; Huang, S.; Chen, X.; Guo, Y.; Lin, Q. The impacts of the East Asian subtropical westerly jet on weather extremes over China in early and late summer. *Atmos. Ocean. Sci. Lett.* **2022**, *15*, 100212. [CrossRef]
38. Yang, X.; Zeng, G.; Zhang, G.; Li, J.; Li, Z.; Hao, Z. Interdecadal Variations of Different Types of Summer Heat Waves in Northeast China Associated with AMO and PDO. *J. Clim.* **2021**, *34*, 7783–7797. [CrossRef]
39. Zhou, F.; Zhang, R.; Han, J. Relationship between the Circumglobal Teleconnection and Silk Road Pattern over Eurasian continent. *Sci. Bull.* **2019**, *64*, 374–376. [CrossRef]

Disclaimer/Publisher's Note: The statements, opinions and data contained in all publications are solely those of the individual author(s) and contributor(s) and not of MDPI and/or the editor(s). MDPI and/or the editor(s) disclaim responsibility for any injury to people or property resulting from any ideas, methods, instructions or products referred to in the content.